

# OpenFoam Final Project

---

## Simulating Supersonic, Inviscid Flow Over A Thin Diamond Airfoil

---

By: Trey Gower, David Valenzano, Ty Zimmerman (group 10)

May 6, 2024

Introduction to Computational Fluid Dynamics  
Fabrizio Bisetti

## SECTION 1: INTRODUCTION & OBJECTIVE

---

The objective of this project is to characterize the lift and drag performance of thin diamond-shaped airfoils under supersonic conditions in inviscid flow using rhoCentralFoam. Under inviscid assumptions, drag is typically assumed to not occur due to D'Alembert's paradox in inviscid flow. However, from the compressibility effects of supersonic flows, wave drag arises from the formation of shocks on the surface of the airfoil. In order to accentuate the effects of wave drag and simplify our simulations, a thin diamond airfoil was selected for study to eliminate the leading edge drag caused by a detached bow shock. To determine the lift performance, this project examined a range of angles of attack throughout the simulations. Similarly, in order to determine convergence, we tested meshes of different refinements to confirm the accuracy of the results. Finally, our results were compared to the existing wind tunnel research regarding supersonic flow around a diamond airfoil to corroborate the findings.

Nomenclature:

C_l	Lift Coefficient, Lift/qS
C_d	Drag Coefficient, Drag/qS
$\alpha$	Angle of Attack, deg
M	Mach number
L/D	Lift to drag ratio
p	Static pressure
u	Free-Stream velocity
L_f	Length of region in front of airfoil
L_w	Length in region in wake of airfoil
H	Height above/below airfoil

## SECTION 2: SETUP

---

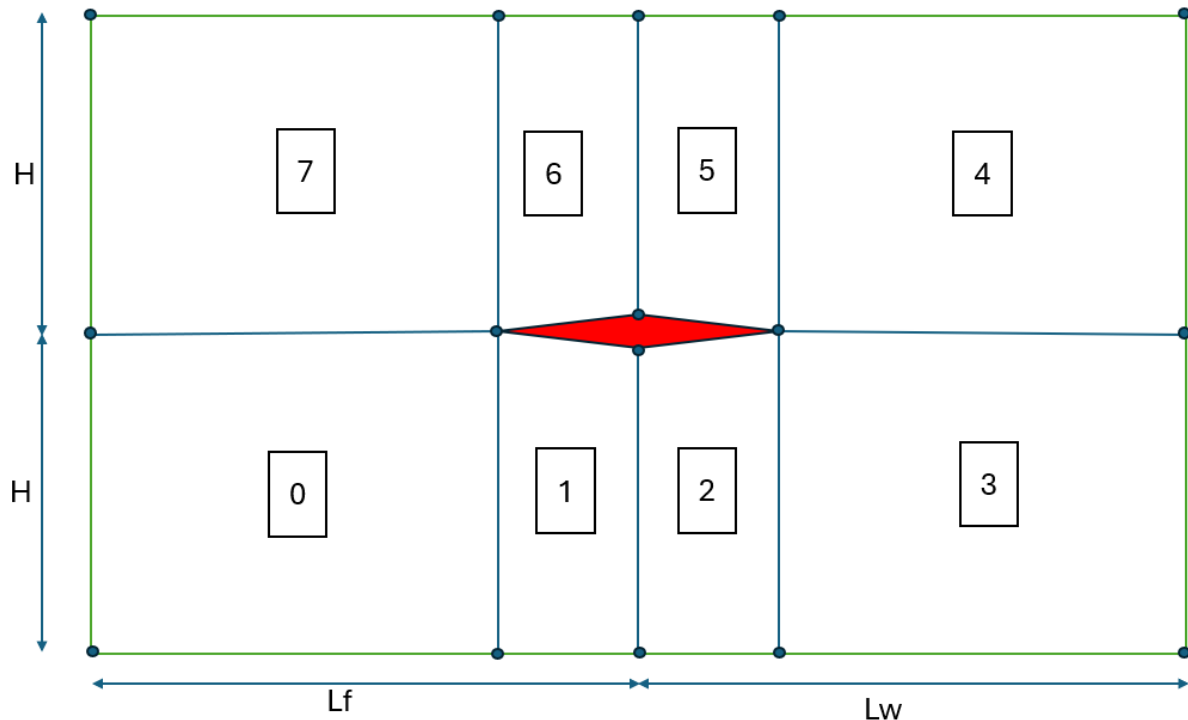


*Figure 1: Schematic of Mesh, blocks and vertices*

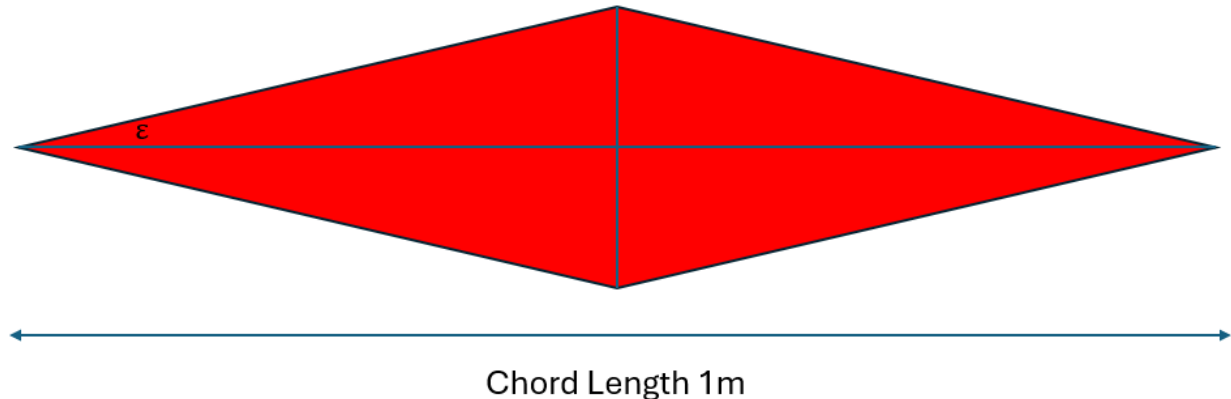


*Figure 2: Diamond Airfoil, with leading edge turning angle ' $\epsilon$ '*

The initial mesh was generated according to Figure 1.  $L_f$  and  $L_w$  represent the length of the regions in front of and behind the half chord of the airfoil respectively, and  $2H$  is the total height of the mesh with  $H$  above and below the airfoil. The turning angle ( $\epsilon$ ) was chosen to be  $3.433^\circ$  for simplicity of comparison to established research. For the same reason, the thickness to

chord ratio is 0.06. The same setup using rhoCentralFoam from project 3 was implemented such that the Mach number could be controlled by just changing the incoming freestream velocity to the desired Mach number while still keeping the specific heat that of air at 1.4. The pressures along the surfaces of the airfoil will then be probed to see if they match predicted solutions from analytical methods and to identify the drag and lifting qualities of the airfoil under multiple angles of attack.

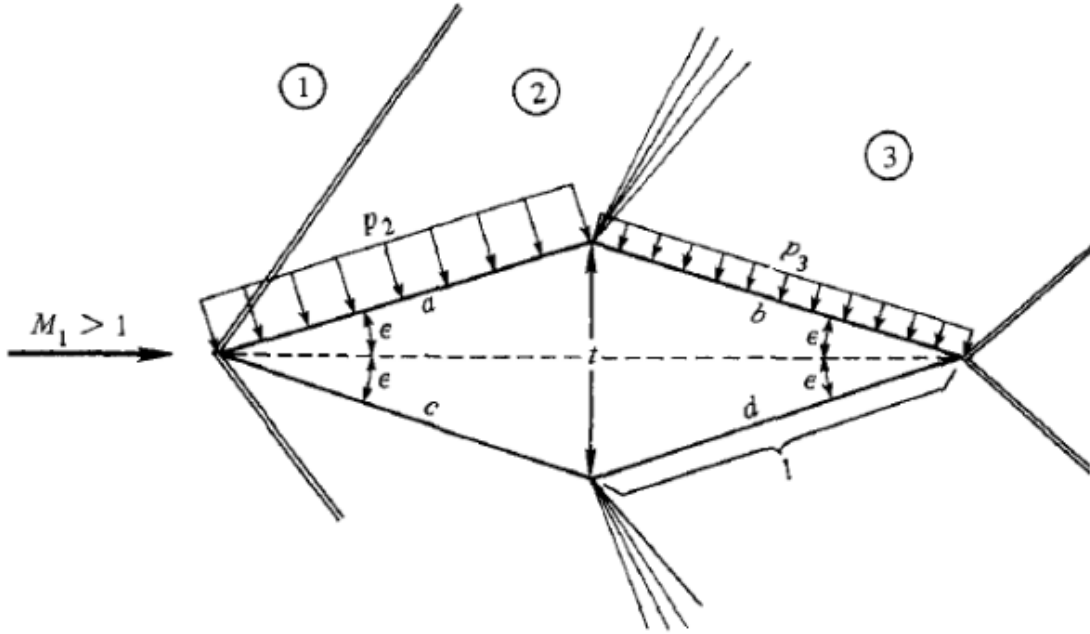


**Figure 3: Schematic of diamond airfoil in supersonic flow and expected shock and fan formation**

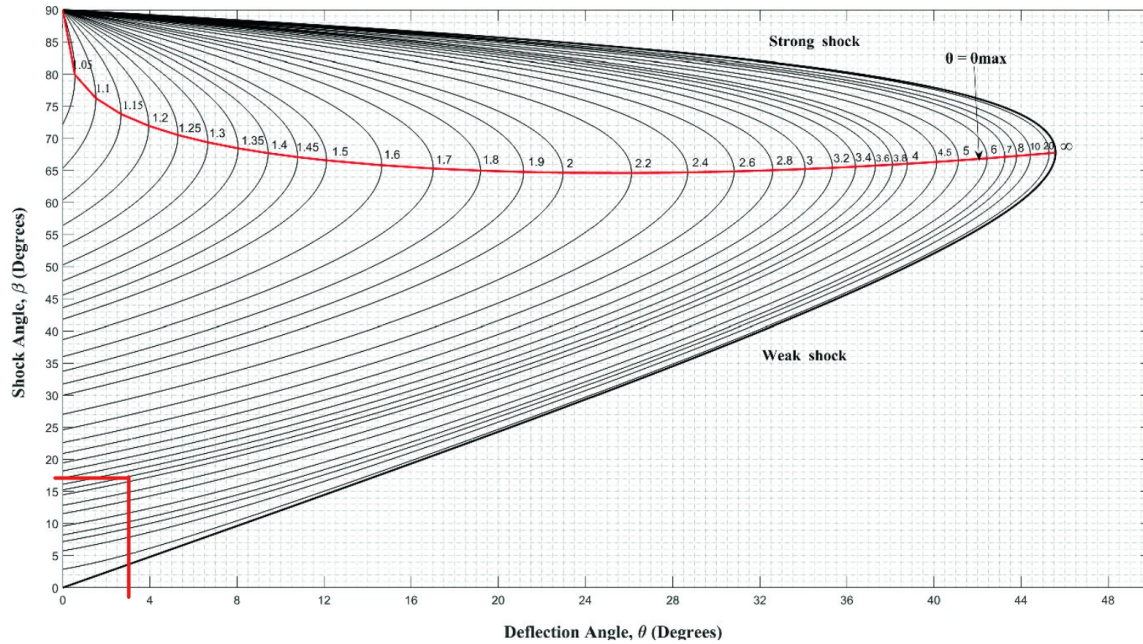


**Figure 4:  $\theta$ - $\beta$ - $M$  curve, with prediction for initial tests**

$$\tan(\theta) = 2 \cot(\beta) \frac{M_1^2 \sin^2(\beta) - 1}{M_1^2 (\gamma + \cos(2\beta)) + 2} \quad (\text{eq. 1})$$

where:

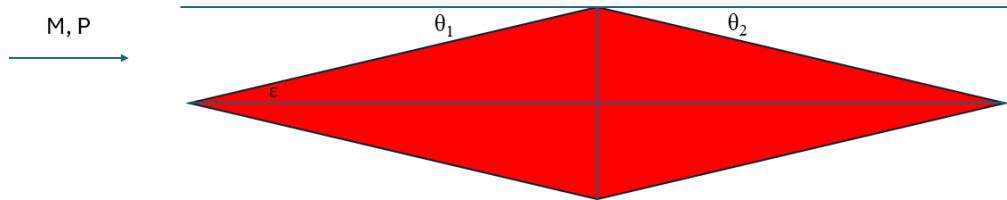
$\theta$  = the angle between the surface of the airfoil and the direction of unaltered airflow

$\beta$  = angle between shock wave and the direction of unaltered airflow

$M_1$  = Mach number of the unaltered airflow

**Figure 5: Equation for deflection angle, shock angle**

In order to study shock behavior, we used the oblique shock relationships given in figures 4 and 5 above. For the test case of zero angle of attack, the turn angle of 3.4 degrees is shown in red depicting that the simulation should show a shock emanating from the tip at approximately 17 degrees. In this study the flow's turning angle will be changed by changing the angle of attack of the airfoil. Prandtl-Meyer Expansion Fan relations will rather be used at higher angles of attack and for the midsection, in which the edge is an expansion fan rather than an oblique shock. Tables from Anderson<sup>[2]</sup> were used for analytical solutions to the Oblique Shock Relations and Prandtl-Meyer expansion fan equations for the pressures along a streamline over the surface of the airfoil. Finally, an expression from inviscid theory will be employed to calculate the lift and drag coefficients for the airfoil.



$$C_l = \frac{1}{\cos(\epsilon)} \frac{1}{\gamma M^2} \left[ \left( \frac{P_3}{P} \cos(\theta_2) + \frac{P_4}{P} \cos(\theta_1) \right) - \left( \frac{P_1}{P} \cos(\theta_1) + \frac{P_2}{P} \cos(\theta_2) \right) \right]$$

$$C_d = \frac{1}{\cos(\epsilon)} \frac{1}{\gamma M^2} \left[ \left( \frac{P_1}{P} \sin(\theta_1) + \frac{P_3}{P} \sin(\theta_2) \right) - \left( \frac{P_2}{P} \sin(\theta_2) + \frac{P_4}{P} \sin(\theta_1) \right) \right]$$

**Figure 6: Naming Convention and Expressions for Lift and Drag Coefficients**

## SECTION 3: BEHAVIOR OF THE SYSTEM (RESULTS)

---

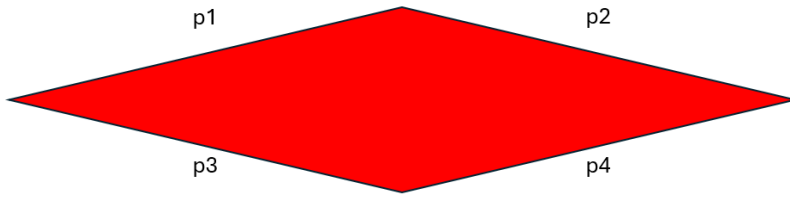


*Figure 7: Nomenclature of Each Surface's Pressure*

### Pressure on each surface of the diamond

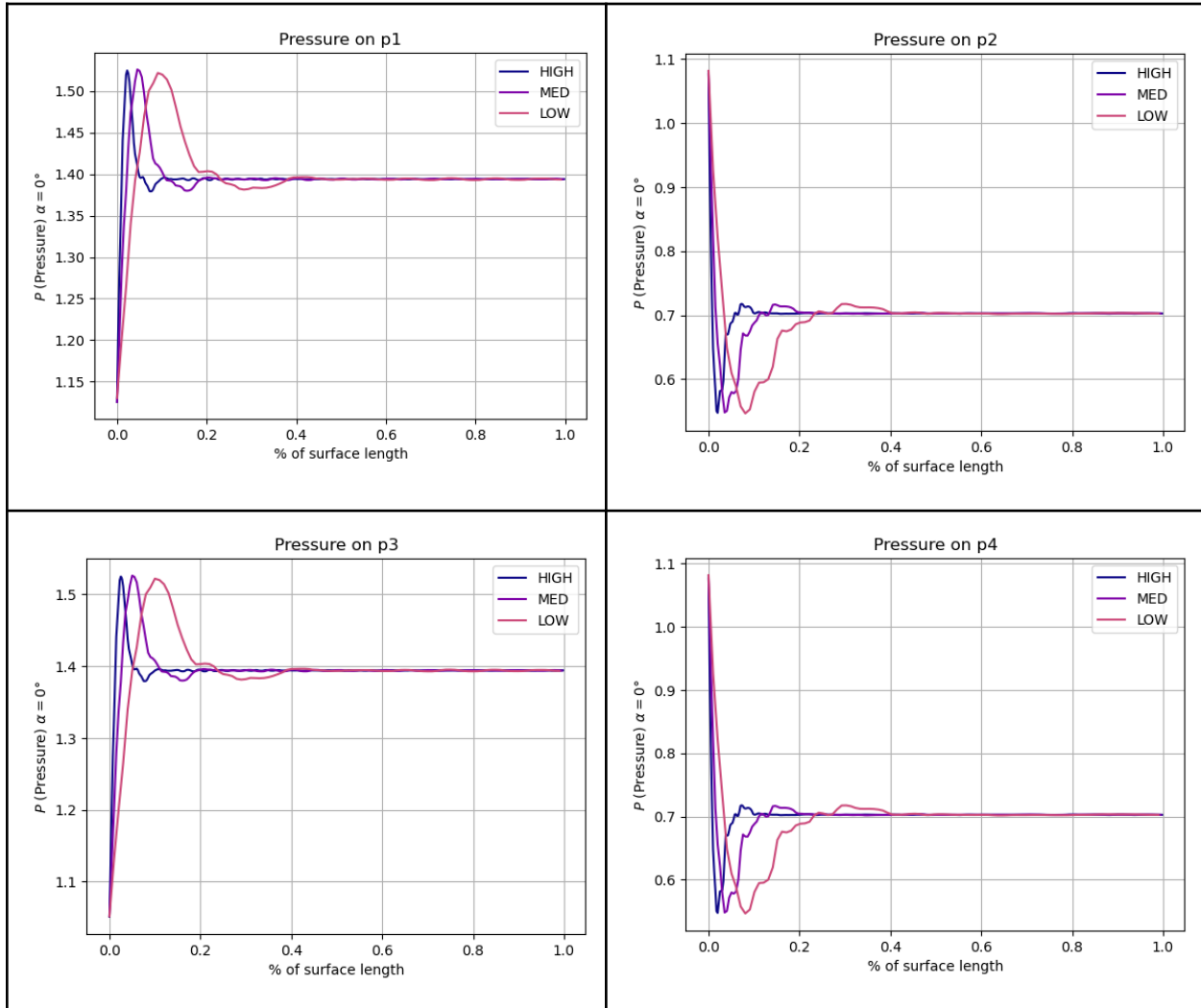


*Figure 8: Pressure at  $\alpha = 0^\circ$  for increasingly refined meshes*

**Table 1: Average pressure on each surface of the diamond  $\alpha = 0^\circ$**

$n = \# \text{ of cells}, \Delta t = \text{time step}$

<u>Average Pressure</u>	<u>Low</u> n = 200,000 $\Delta t = 0.00016 \text{ s}$	<u>Med</u> n = 800,000 $\Delta t = 0.00008 \text{ s}$	<u>High</u> n = 2,560,000 $\Delta t = 0.00004 \text{ s}$	<u>Analytical Solution</u>
p1	1.397	1.396	1.395	1.394
p2	0.6972	0.6999	0.7012	0.703
p3	1.394	1.394	1.394	1.394
p4	0.7019	0.7035	0.6988	0.703

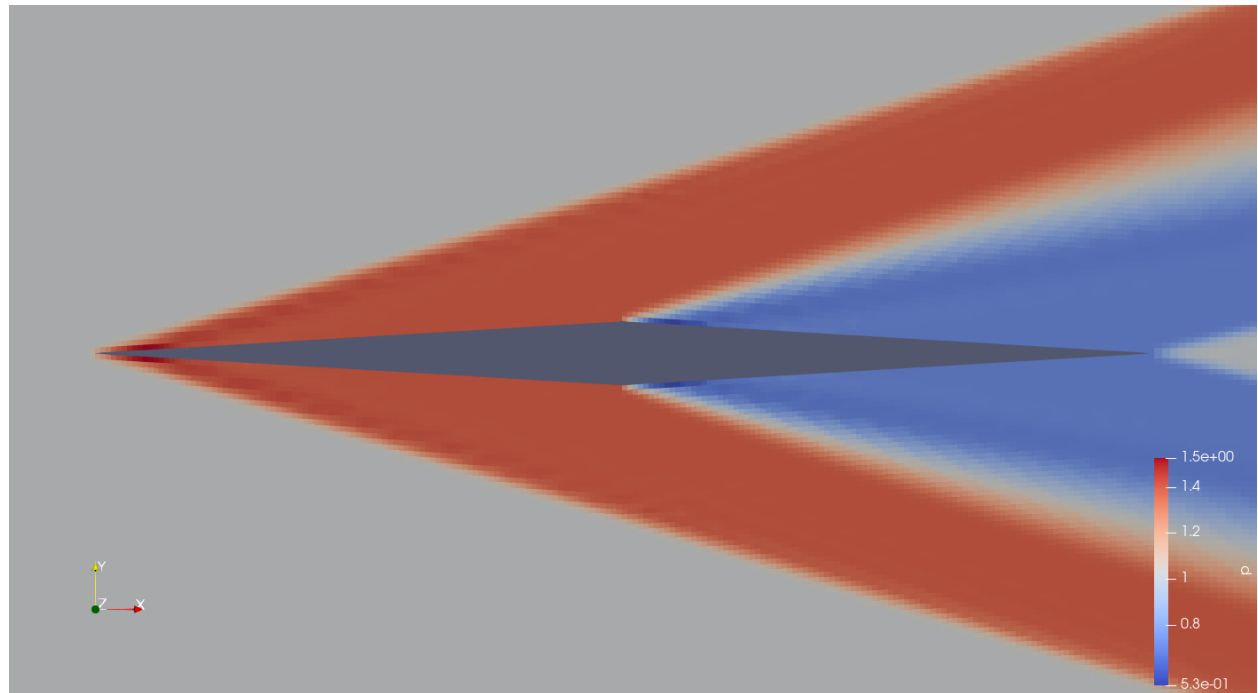


*Figure 9: Low Resolution Zero Angle of Attack*

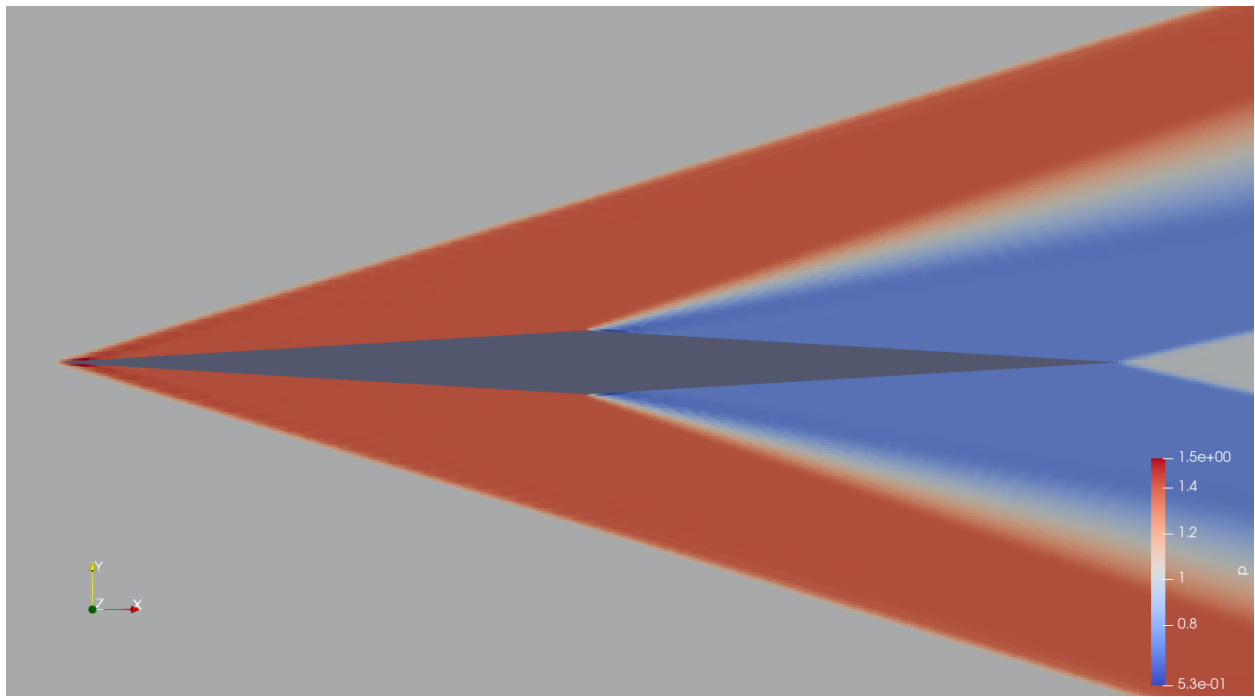


*Figure 10: Medium Resolution Zero Angle of Attack*

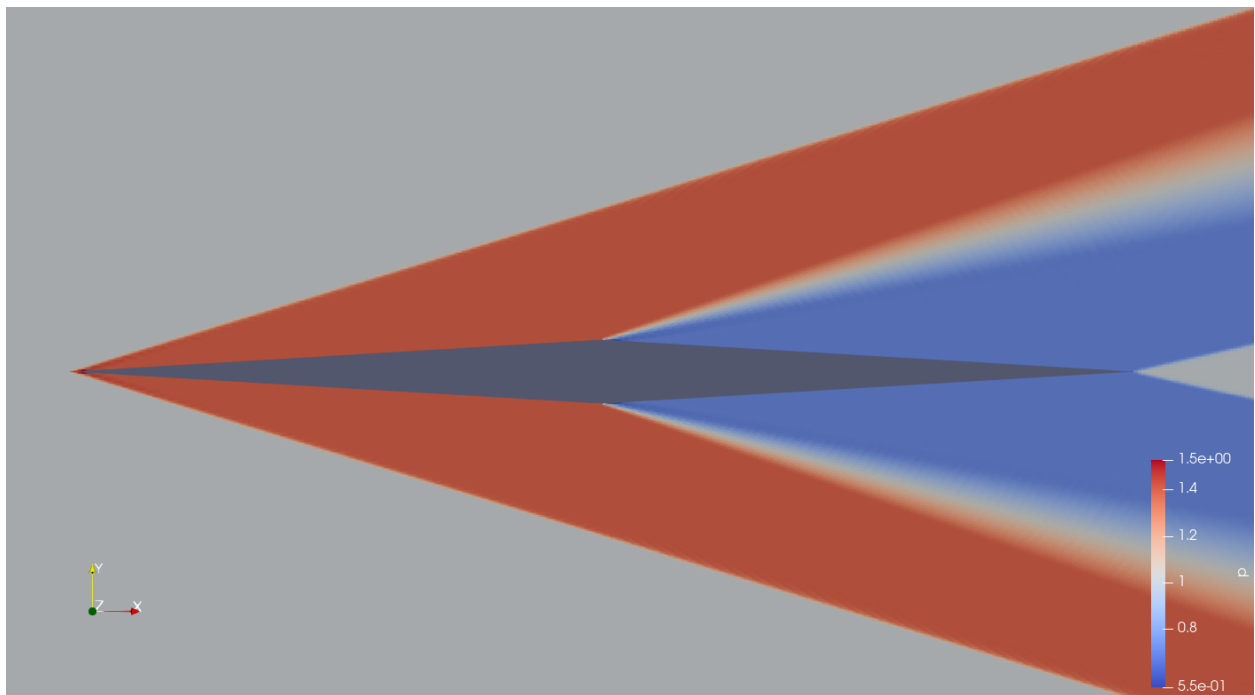


*Figure 11: High Resolution Zero Angle of Attack*

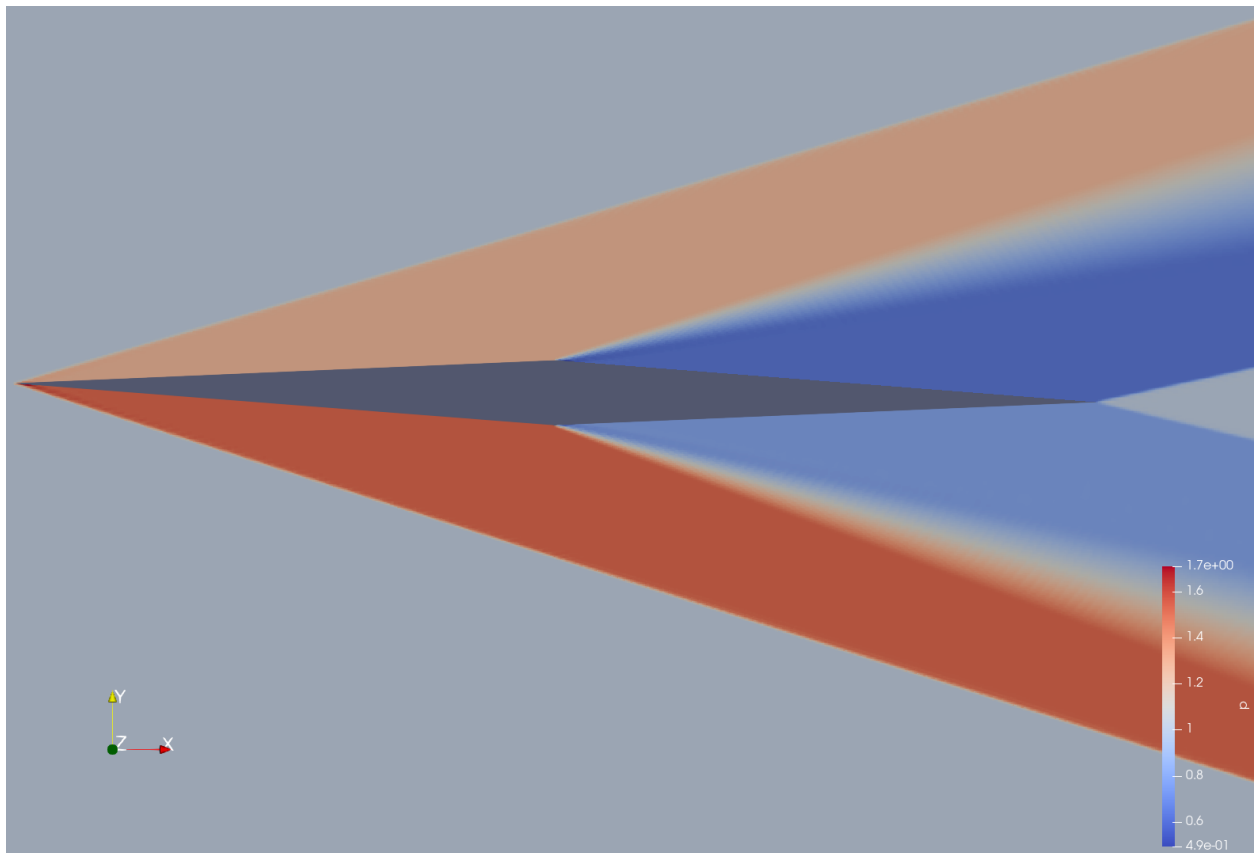


Figure 12: High Resolution  $\alpha = 1^\circ$

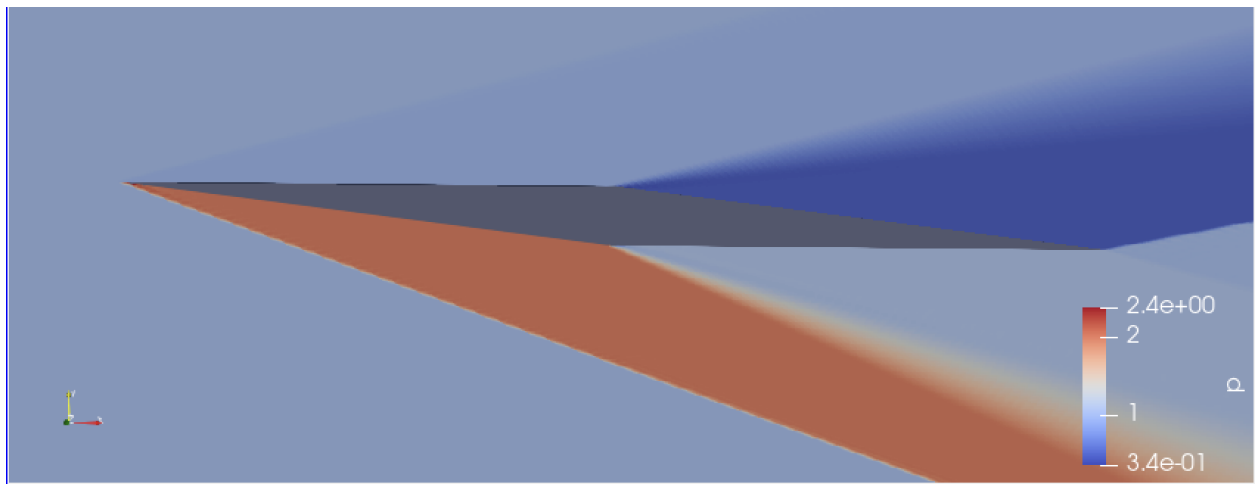
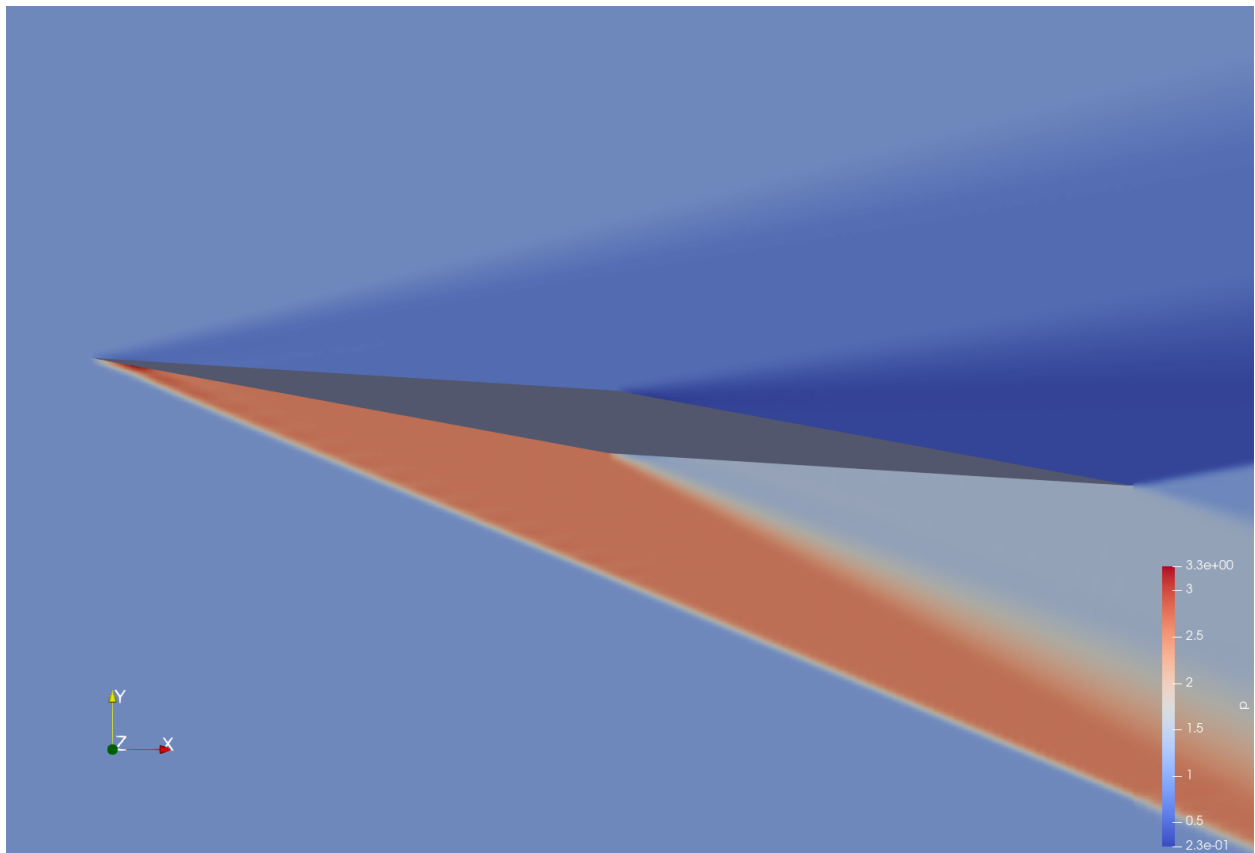
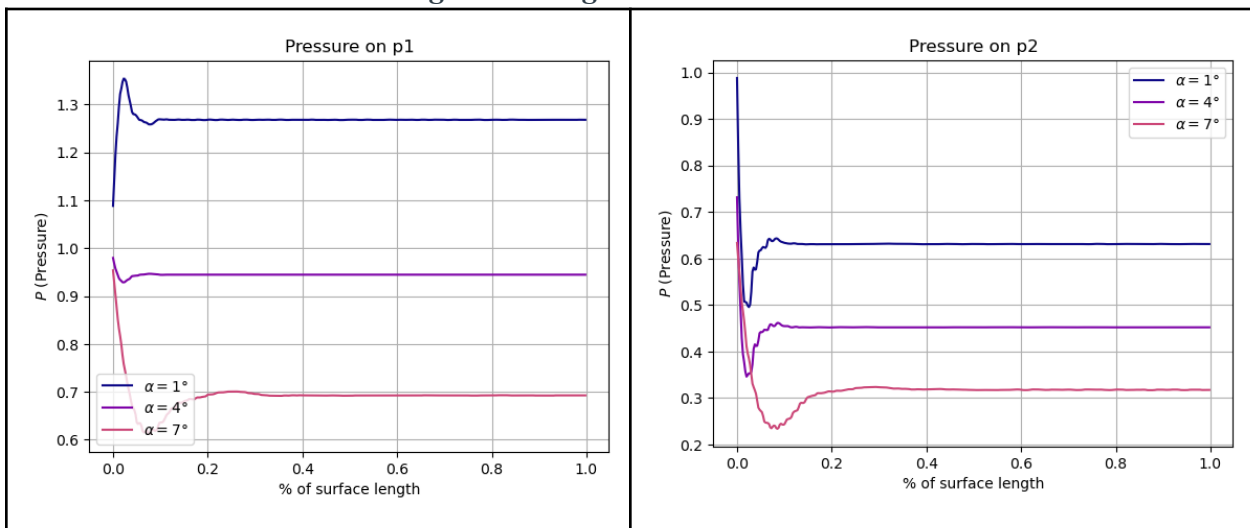
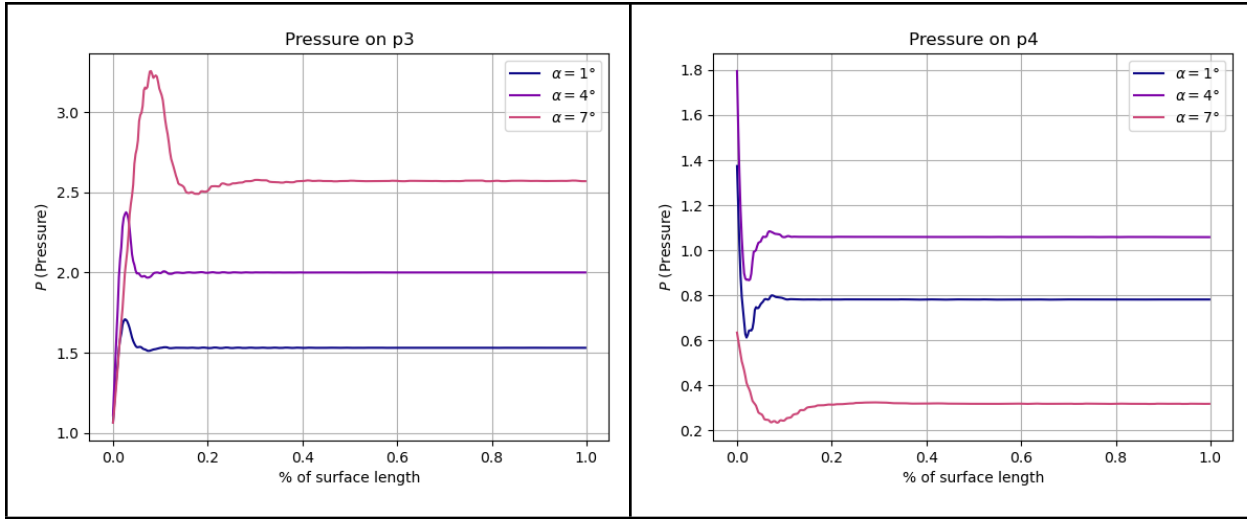


Figure 13: High Resolution  $\alpha = 4^\circ$



*Figure 14: High Resolution  $\alpha = 7^\circ$*





*Figures 15: Pressure on each surface at various angles of attack on the high resolution mesh*

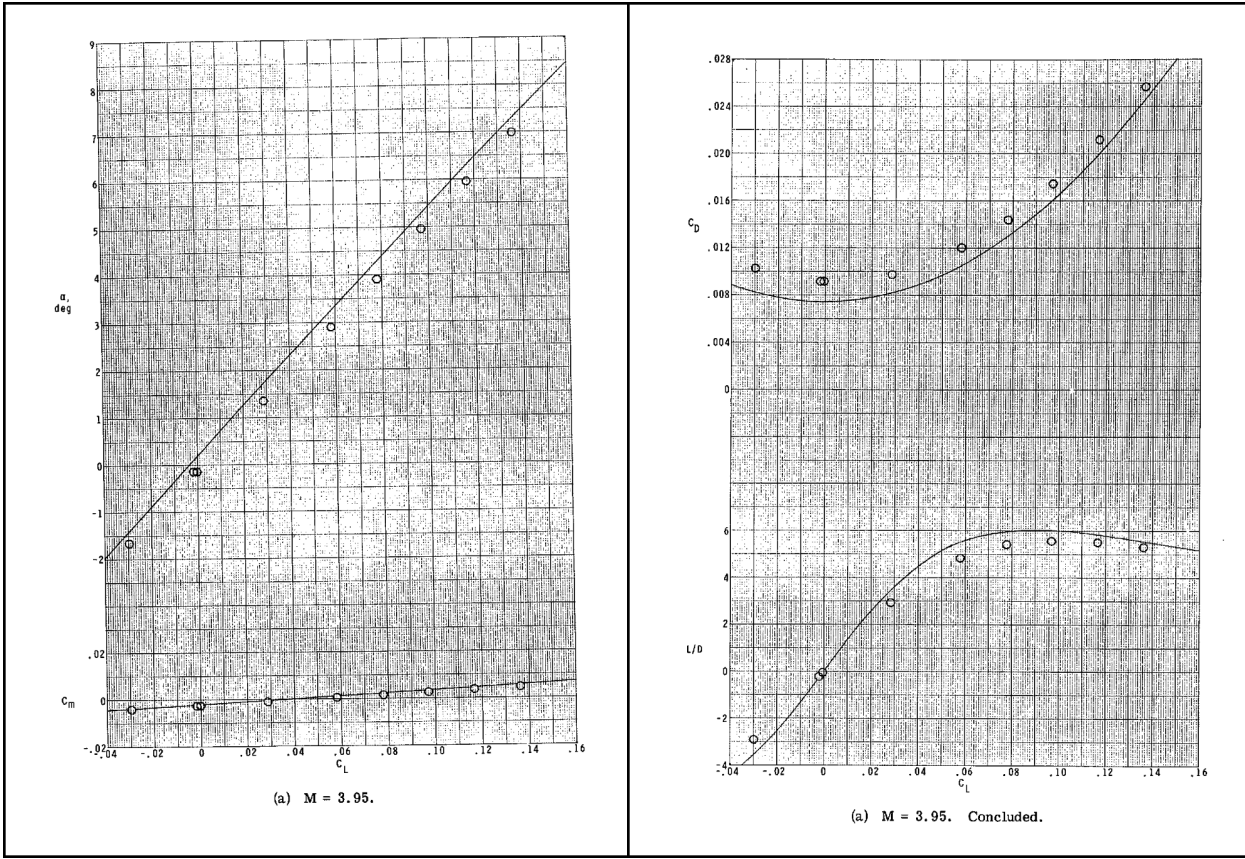
**Table 2: Average pressure on each surface for various angles of attack**

Average Pressure	$\alpha = 1^\circ$	$\alpha = 4^\circ$	$\alpha = 7^\circ$
p1	1.268	0.9446	0.6917
p2	0.6299	0.4511	0.3168
p3	1.529	1.999	2.568
p4	0.7806	1.058	1.424

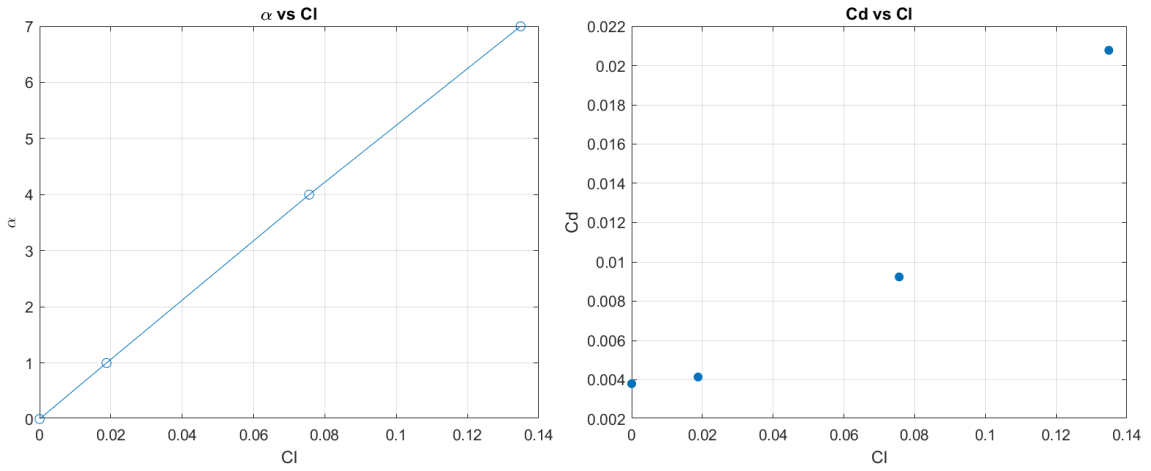
## SECTION 4: COMPARING TO RESEARCH

---

Our point of comparison comes from a series of NASA experiments from June 1974 regarding '[Comparisons of two dimensional shock expansion theory with experimental aerodynamic data for delta planform wings at high supersonic speeds](#)'. From these experiments, qualities of a diamond airfoil wing were gathered and will be compared to the qualities of our diamond airfoil. Making our airfoil shape and Mach number similar to theirs was the reasoning behind the particular 3.433 degree turn angle and 3.95 Mach number, so that our diamond airfoil would match the t/c and tunnel conditions of theirs.



**Figures 16 & 17: Experimental research from Jernell, NASA at  $M = 3.95$  with the same diamond airfoil as used in this study. Left:  $C_L$  v.  $\alpha$ , Right:  $C_L$  v.  $C_D$**



**Figures 18 & 19: CFD Simulation Results at  $M = 3.95$ . Left:  $C_L$  v.  $\alpha$ , Right:  $C_L$  v.  $C_d$**

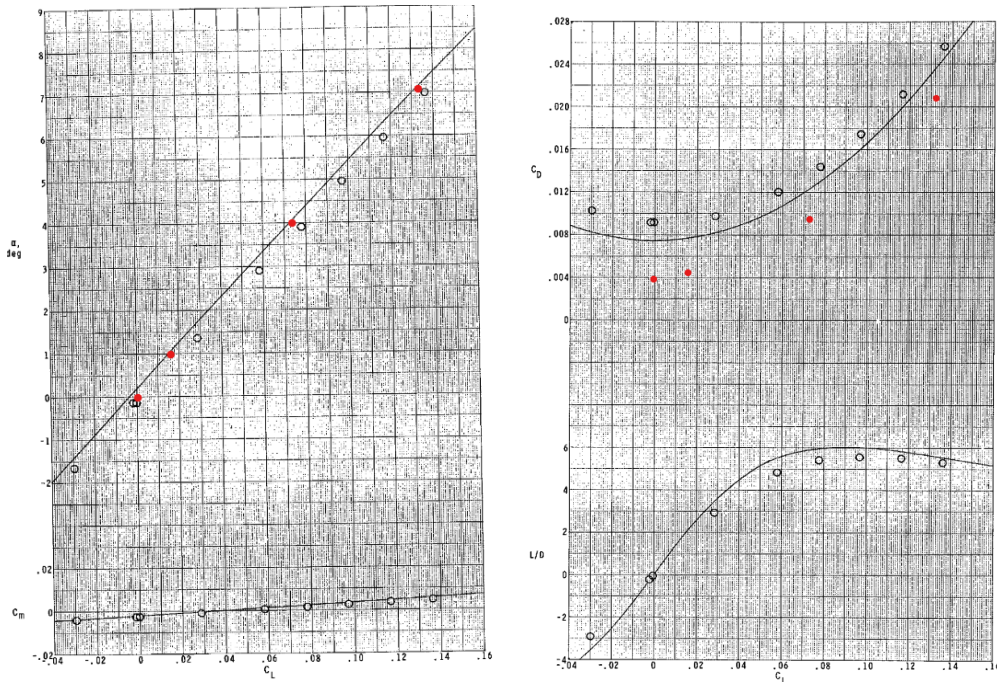
## SECTION 5: ANALYSIS

---

Firstly, the initial prediction from the  $\theta$ - $\beta$ -Mach curve was a 17 degree shock angle for the zero angle of attack and all resolutions were perfectly in line with that prediction. It was noticed that

in the low resolution simulation that a small patch of high or low pressure was appearing at the front of airfoil section surfaces. This can be seen both in the plots and the simulation screenshots, the deep red and deep blue spots. This was strange as the theory predicted uniform pressure over each surface. As the meshes were refined this small patch got smaller and smaller showing that this error was diminishing and the simulation was getting closer to the analytical theory with increasing cell count. Ignoring the high and low patches, the areas with steady pressure for all resolutions are right at the predicted pressures of 1.4 and 0.7. This was important in validating the simulation. The averaged values then also approached the analytical solutions across the resolutions.

An important distinction in our results compared to the NASA research was the fact that they were using a 3-D delta wing and calculating  $C_L$  and  $C_D$ , meanwhile with our 2-D airfoil simulations we're able to calculate  $C_l$  and  $C_d$  respectively. Additionally, our simulations were run under inviscid conditions and the real life wind tunnel will obviously have viscous effects among other considerations for wing geometry and sensor applications. Below are our results superimposed onto NASA's graphs. However, our alpha vs  $C_l$  curve was rather close to their results, just slightly overpredicting. The  $C_d$  vs  $C_l$  curve was understandably, underpredicting. That is, viscous effects would be a large contributing factor to the performance and this can be seen in this result. In a next iteration, it would be an interesting endeavor to use a viscous solver to see if the wind tunnel conditions can be matched and then those simulations compared.



**Figures 20 & 21: Simulation Left:  $C_l$  v.  $\alpha$ , Right:  $C_l$  v.  $C_d$  Superimposed onto Experimental research from Jernell**

## REFERENCES

---

- ANDERSON. (2016). Fundamentals of Aerodynamics (6th ed.). McGraw-Hill Education.
- Bisetti, Fabrizio. "Intro to Computational Fluid Dynamics (COE 347)". University of Texas at Austin. Austin, Texas
- Jernell, Lloyd S. "NASA TN 0-7583." COMPARISONS OF TWO-DIMENSIONAL SHOCK-EXPANSION THEORY WITH EXPERIMENTAL AERODYNAMIC DATA, ntrs.nasa.gov/api/citations/19740018331/downloads/19740018331.pdf. Accessed 5 May 2024.